

**Supplementary Information to “Experimental chemical budgets
of OH, HO₂ and RO₂ radicals in rural air in West-Germany
during the JULIAC campaign 2019”**

Changmin Cho¹, Hendrik Fuchs¹, Andreas Hofzumahaus¹, Frank Holland¹, William J. Bloss³,
Birger Bohn¹, Hans-Peter Dorn¹, Marvin Glowania¹, Thorsten Hohaus¹, Lu Liu¹, Paul S.
Monks², Doreen Niether¹, Franz Rohrer¹, Roberto Sommariva^{2,3}, Zhaofeng Tan¹, Ralf Tillmann¹,
Astrid Kiendler-Scharr¹, Andreas Wahner¹, and Anna Novelli¹

¹Forschungszentrum Jülich, Institute of Energy and Climate Research: Troposphere (IEK-8), Jülich,
Germany

²Department of Chemistry, University of Leicester, Leicester, UK

³School of Geography, Earth and Environmental Sciences, University of Birmingham, Birmingham, UK

Correspondence to: Hendrik Fuchs (h.fuchs@fz-juelich.de) and Anna Novelli (a.novelli@fz-juelich.de)

Table S1. HO₂ and RO₂ background signals converted into apparent ambient concentrations used in the evaluation of HO₂ and RO₂ measurements. The average background signals originate from the reference experiments in the chamber while the upper limits are obtained from calibrations.

	HO ₂ background 10 ⁷ cm ⁻³	HO ₂ background upper limit 10 ⁷ cm ⁻³	RO ₂ background 10 ⁷ cm ⁻³	RO ₂ background upper limit 10 ⁷ cm ⁻³
Winter	0.4±0.6	1.2	0.5±0.2 2.8±0.4 ^a	2.8
Spring	1.0±0.15	2.0	0.5±0.2	2.5
Summer	1.0±0.6	2.1	2.8±0.5	5.4
Autumn	0.0±0.4	1.5	0.0±0.4	1.5

^a Variable background signals that are equivalent to RO₂ concentrations: from 14 Jan. to 25 Jan.: $(0.5 \pm 0.2) \times 10^7 \text{ cm}^{-3}$, from 26 Jan. to 6 Feb.: $(1.6 \pm 0.2) \times 10^7 \text{ cm}^{-3}$, from 07 Feb. to 10 Feb.: $(2.8 \pm 0.4) \times 10^7 \text{ cm}^{-3}$.

Table S2. List of the used VOCs for the radical budget analysis.

Classification	Species	Instrument
alkenes	pentene, hexene	VOCUS- PTR-TOF-MS
aromatics	toluene, xylene, benzene, phenol, furan, styrol, cresol	PTR-TOF-MS
BVOCs	isoprene, monoterpenes, sesquiterpenes	VOCUS- PTR-TOF-MS
OVOCs	acetaldehyde, acetone, acetonitrile, acrolein, adipinic acid, benzaldehyde, butanone, cyclohexanone, formic acid, glycolaldehyde, glycolic acid, hydroxyacetone, methylglyoxal, methyl vinyl ketone, methacrolein, nopinone, pentanone, pinonaldehyde, succinic acid	VOCUS- PTR-TOF-MS

36 **Table S3.** Meteorological and trace gas conditions during the specific period for Case 1 and 2.

Parameter	Case 1 (05.08 - 08.08.2019)		Case 2 (22.08 - 31.08.2019)	
	Median	Interquartile	Median	Interquartile
SAPHIR				
temperature (°C)	27.0	7.8	31.0	9.1
H ₂ O (%)	1.44	0.25	1.4	0.5
OH (10 ⁶ cm ⁻³)	4.5	5.2	4.1	5.7
HO ₂ (10 ⁸ cm ⁻³)	1.4	1.4	2.7	3.8
RO ₂ (10 ⁸ cm ⁻³)	2.1	2.6	2.9	3.1
O ₃ (ppbv)	37.5	11.3	57.5	37.6
NO (ppbv)	0.26	0.39	0.22	0.54
NO ₂ (ppbv)	3.4	2.2	4.3	4.6
CO (ppmv)	0.12	0.01	0.16	0.03
HCHO (ppbv)	1.8	0.7	3.4	1.8
HONO (ppbv)	0.18	0.09	0.21	0.15
<i>k</i> _{OH} (s ⁻¹)	5.2	1.1	8.7	3.4
<i>k</i> _{VOC} (s ⁻¹)	3.3	0.9	5.7	3.4
Total aerosol surface area (10 ⁷ nm ² cm ⁻³)	8.5	2.5	11.2	11.7

37

38

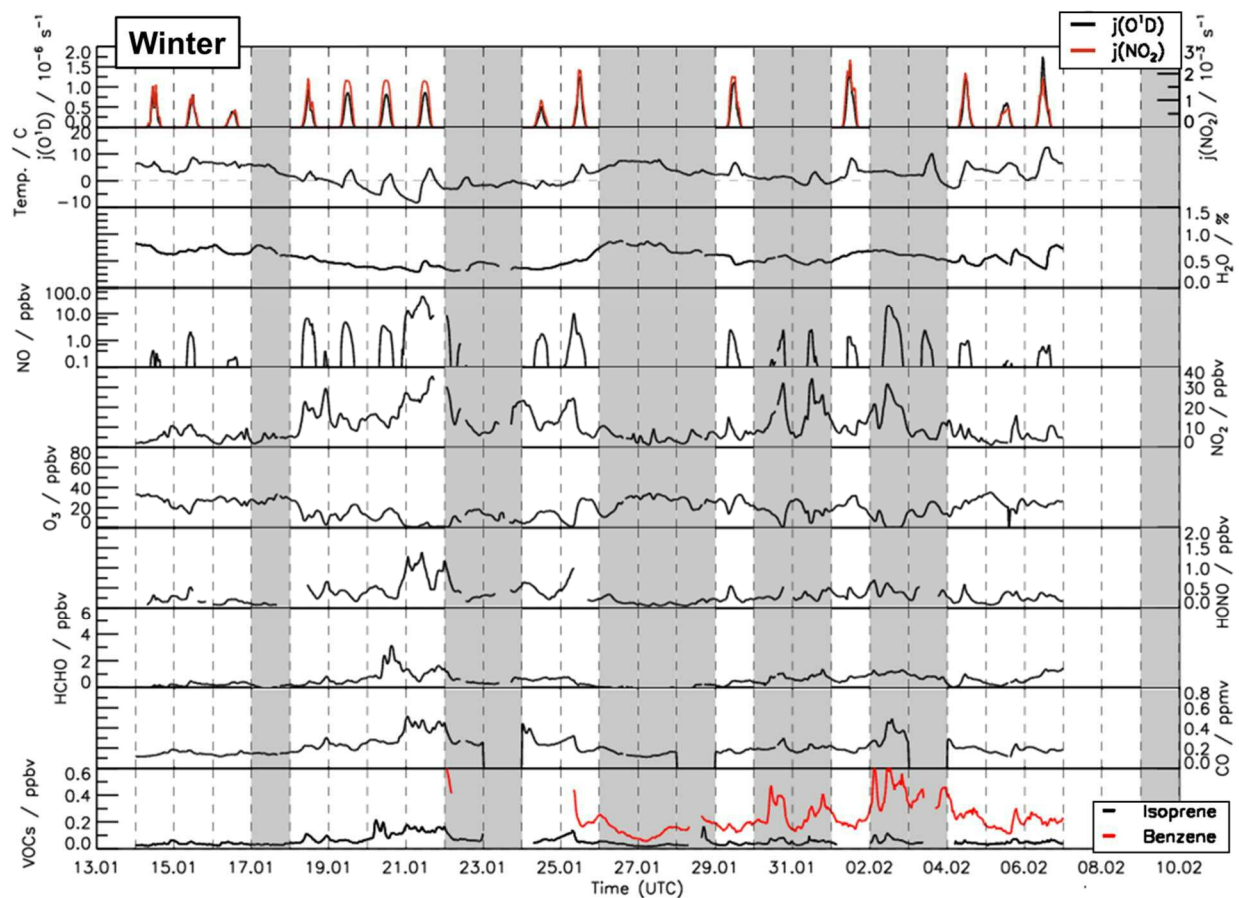


Figure S1: Time series of temperature and trace gas concentrations during the winter period of the JULIAC campaign (Cho et al., 2022). Vertical dashed lines denote midnight. Grey shaded areas indicate calibration days, when no measurements were done and days when the chamber roof was closed due to bad weather conditions.

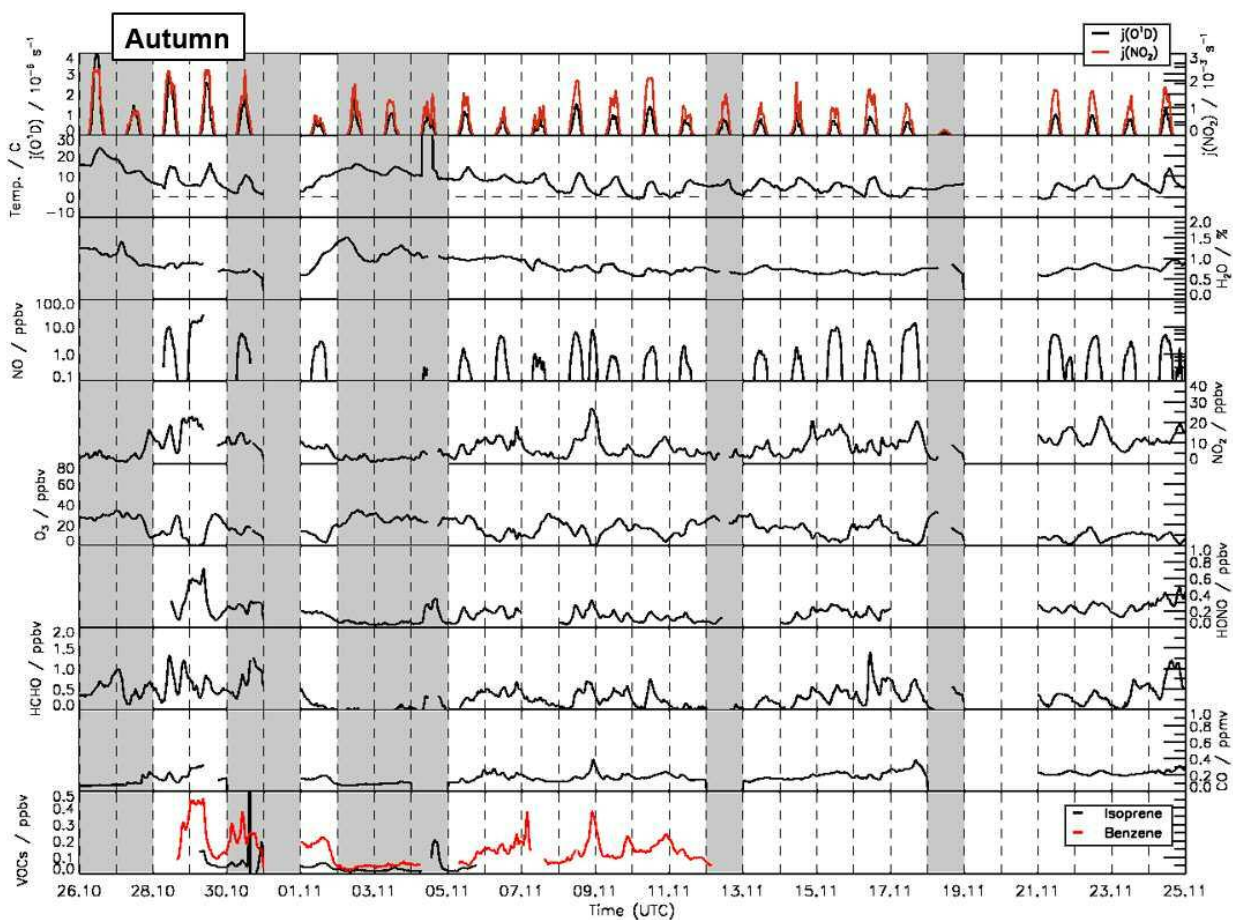


Figure S2: Time series of temperature and trace gas concentrations during the autumn period of the JULIAC campaign (Cho et al., 2022). Vertical dashed lines denote midnight. Grey shaded areas indicate calibration days, when no measurements were done and days when the chamber roof was closed due to bad weather conditions.

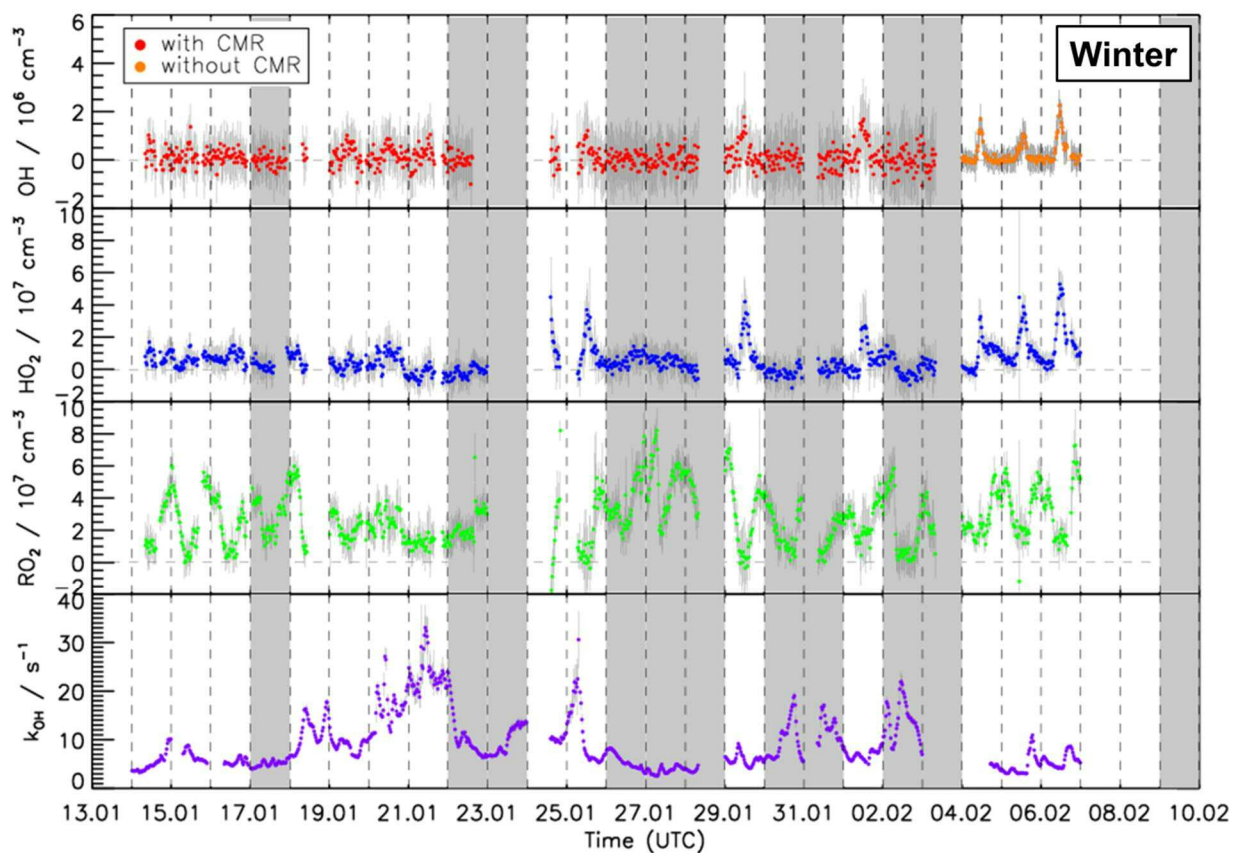
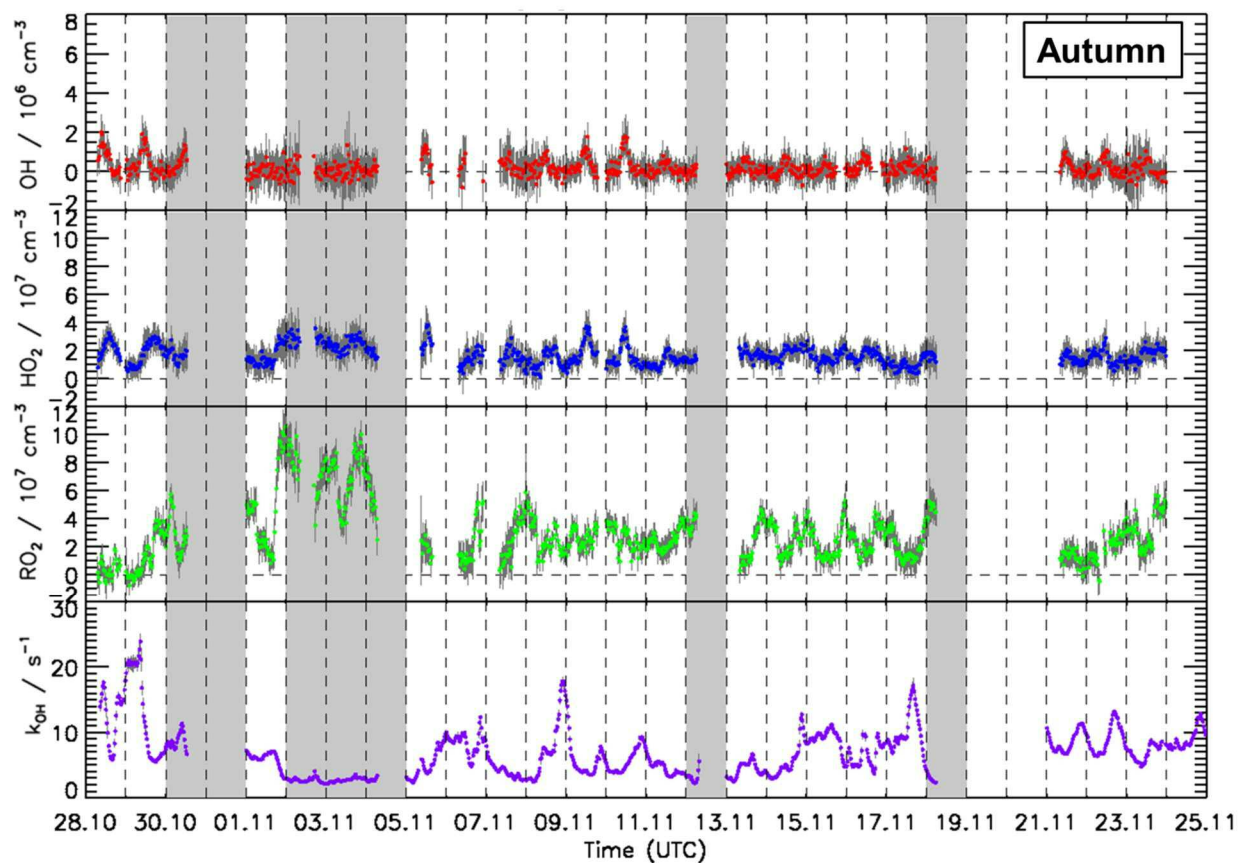
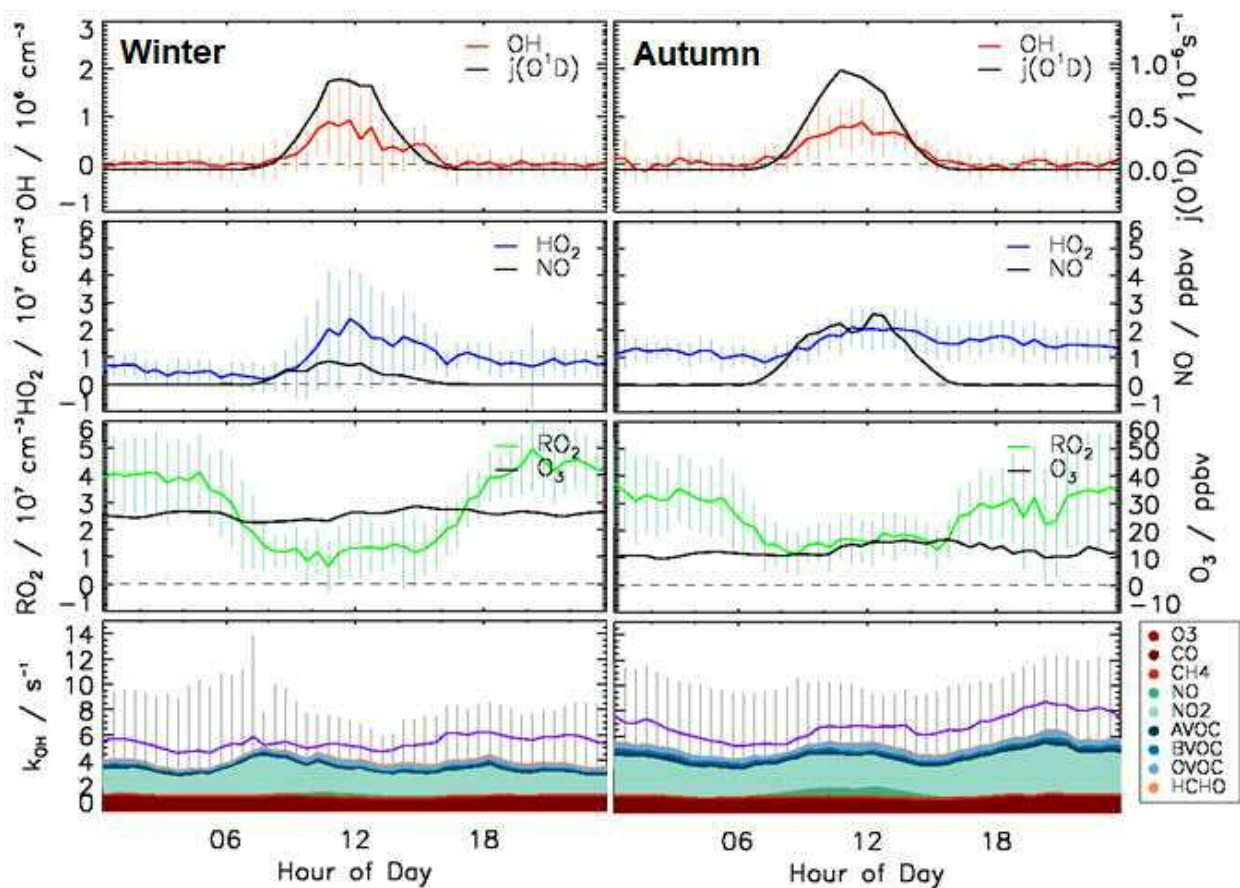


Figure S3: Time series of OH, HO₂, and RO₂ radical concentration measured by the FZJ-LIF-CMR instrument and measurements of the OH reactivity (k_{OH}) measured in the winter period of the JULIAC campaign (Cho et al., 2022). Vertical dashed lines denote midnight. Grey shaded areas indicate calibration days when no measurements were done and days when the chamber roof was closed due to bad weather conditions.



55 **Figure S4:** Time series of OH, HO₂, and RO₂ radical concentration measured by the FZJ-LIF-CMR
 56 instrument and measurements of the OH reactivity (k_{OH}) measured in the autumn period of the JULIAC
 57 campaign (Cho et al., 2022). Vertical dashed lines denote midnight. Grey shaded areas indicate
 58 calibration days when no measurements were done and days when the chamber roof was closed due to
 59 bad weather conditions.



60 **Figure S5:** Median values of the diurnal profiles of OH, HO₂, RO₂, k_{OH} , $j(\text{O}^1\text{D})$, NO, O₃ measured in the
 61 winter and autumn periods of the JULIAC campaign. Colored areas represent the contributions of
 62 measured reactants to the total OH reactivity. Vertical lines give 25th and 75th percentile values.

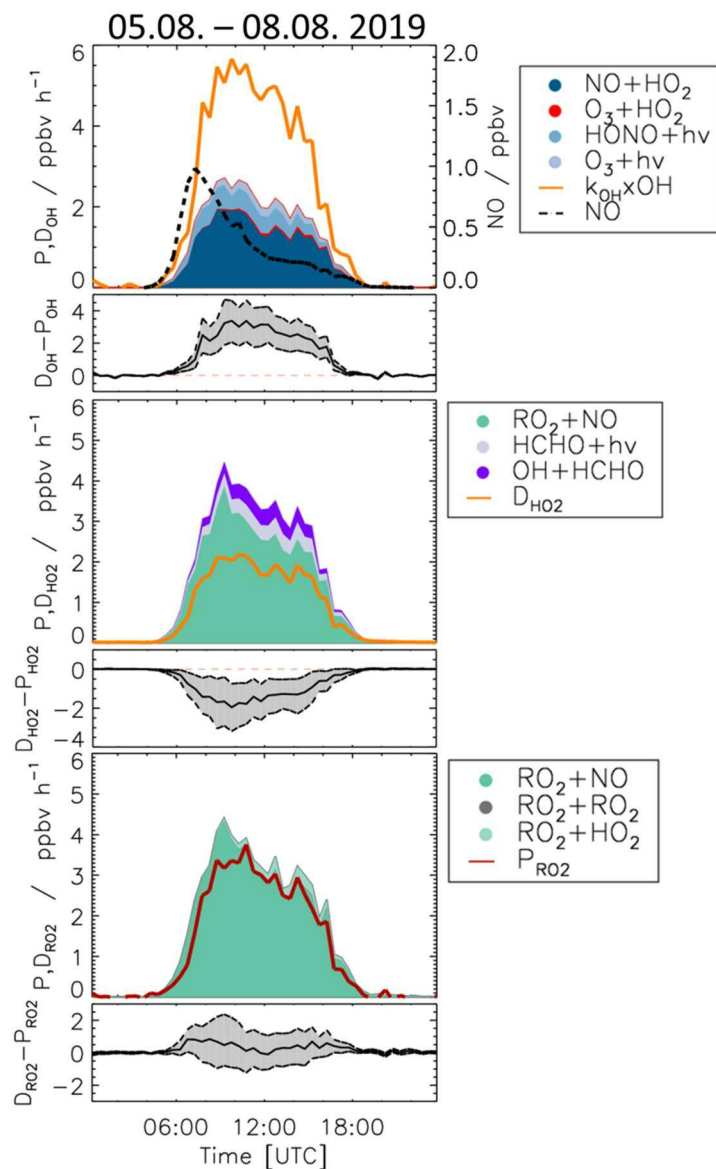


Figure S6: Chemical budgets for OH, HO₂, and RO₂ radicals similar to Figure 12 (only Case 1), using the lower limit of the reaction rate coefficient of the reaction of RO₂ with NO, $7.7 \times 10^{-12} \text{ cm}^3 \text{ s}^{-1}$ (at 298 K for CH₃O₂) to calculate the turnover rate of this reaction.

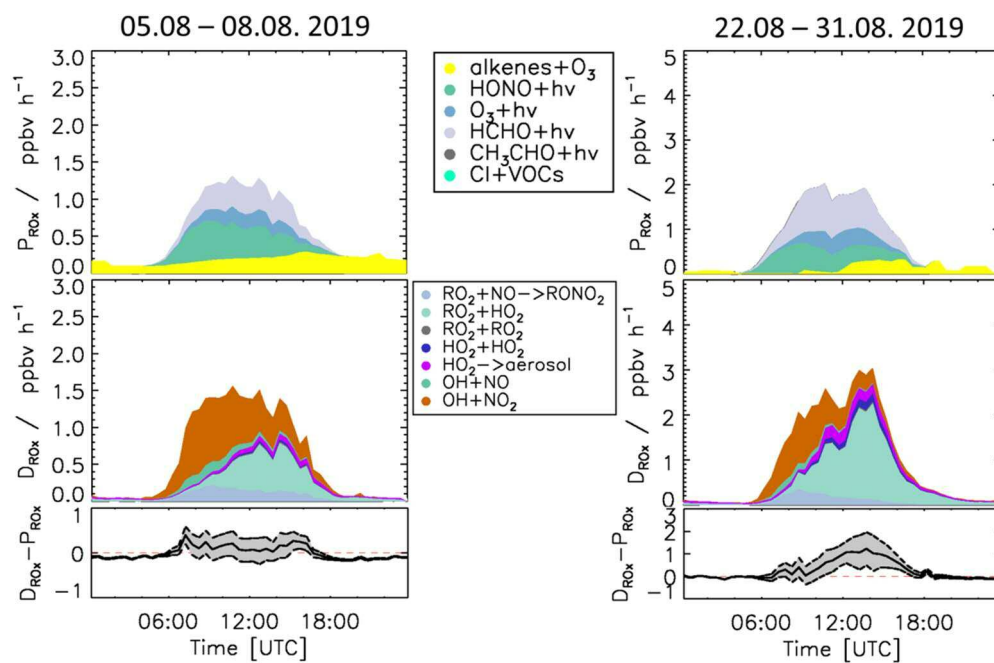


Figure S7: Experimental budgets for RO_x similar to Figure 11 (Case 1 and 2), using the high limits of alkene concentrations contributing to radical production by ozonolysis reactions and applying the HO₂ uptake on the aerosols (Section 4.2).